ARTICLE IN PRESS

Available online at www.sciencedirect.com

SCIENCE DIRECT®

Journal of Magnetic Resonance 167 (2004) 221–227

JMR Journal of Magnetic Resonance

www.elsevier.com/locate/jmr

A longitudinally detected high-field ESR spectrometer for the measurement of spin–lattice relaxation times

Ferenc Murányi, Ferenc Simon,* Ferenc Fülöp, and András Jánossy

Budapest University of Technology and Economics, Institute of Physics and Solids in Magnetic Fields Research Group of the Hungarian Academy of Sciences P.O. Box 91, H-1521, Budapest, Hungary

Received 10 October 2003; revised 21 November 2003

Abstract

We describe a high-field longitudinally detected electron spin resonance (LOD-ESR) spectrometer operating at 35 and 75 GHz. The lack of resonant microwave circuits facilitates operation at different microwave frequencies without changing the probehead. A very low noise radio frequency detection compensates partially the resulting low sensitivity. The major elements of the LOD-ESR spectrometer are commercially available and may be adapted to usual high frequency spectrometers. The instrument allows field and frequency dependent spin lattice relaxation time (T_1) studies. T_1 in the range of 2–80 ns can be determined from the phase sensitively detected LOD-ESR spectra. We demonstrate the performance of the apparatus by the measurement of T_1 in the normal state of RbC_{60}, an electrically conducting alkaline fulleride polymer.

Keywords: High field; ESR; Spin–latttice relaxation; RbC60

1. Introduction

Lately, there is a tendency in electron spin resonance (ESR) instrumentation to use higher magnetic fields with corresponding higher microwave frequencies to obtain higher resolution or for the study of magnetic field dependent phenomena. Recent technical developments in the field of high-field ESR (HF-ESR) are reviewed in [1,2]. There are two distinct approaches in HF-ESR instrumentation: one way is to improve the sensitivity with resonant microwave elements such as the quasi-optical systems utilizing Fabry–Pérot resonators [3–5] or small size cylindrical resonant cavities [3,6]. These instruments are designed for chemical or biological studies, they have a high sensitivity at the cost of operating at a fixed microwave frequency and a limited temperature variability. Another approach is to avoid the use of resonant microwave elements, this enables easy operation at several microwave frequencies in a broad temperature range at the cost of sensitivity. This is better fitted to physical problems in solids where magnetic field and temperature have to be often varied in a broad range [7,8].

Longitudinally detected ESR (LOD-ESR) complements continuous wave (cw) ESR and spin-echo methods as it allows the measurement of short longitudinal relaxation times [9–11] and to separate overlapping ESR signals of spin species [12–15]. The instrument detects the modulation of the longitudinal magnetization, M_z, induced by a chopped microwave field, using a pick-up coil parallel to the external magnetic field, H_0. LOD-ESR apparatus built up to date were based on conventional X-band ESR spectrometers.

Here, we describe the development of a high-field LOD-ESR (HF-LOD-ESR) that combines the HF-ESR and the LOD techniques and operates at 35 and 75 GHz [16]. We do not employ resonant microwave structures so the exciting field intensity at the sample and the detected signals are low. We compensate for the weak signals with a very low noise radio frequency (*rf*) detection system and the use of high chopping frequencies, ranging up to 30 MHz. The apparatus enables the direct determination of the electronic spin

* Corresponding author.
E-mail address: simon@esr1.fkf.bme.hu (F. Simon).

1090-7807/$ - see front matter © 2003 Elsevier Inc. All rights reserved.
doi:10.1016/j.jmr.2003.11.011

lattice relaxation rate T_1 in the 2–80 ns range and is potentially useful for lossy samples. The lack of resonant microwave structures allows multifrequency measurements using the same probehead. Our apparatus demonstrates the feasibility of the HF-LOD-ESR technique for studying magnetic field dependent relaxation phenomena.

In what follows, we outline the principles of the LOD-ESR method and describe the analysis of the LOD-ESR spectrum for the determination of T_1. We describe our experimental apparatus in detail and as an example discuss the spin–lattice relaxation time measurements in the RbC_{60} conducting fulleride polymer.

2. Principles of LOD-ESR

LOD-ESR experiments can be classified into cw and pulsed LOD-ESR techniques. The pulsed version of the LOD-ESR combines pulsed ESR methods with the longitudinal detection. Its main advantage over the usual pulsed ESR methods is the inherent isolation of excitation and detection thus there is no dead time and measurement on timescales shorter than for pulsed ESR is possible. The limitation of this method as compared to continuous LOD-ESR is the relatively low duty cycle of microwave irradiation. Higher microwave powers and resonating structures are necessary for measurement of T_1 or to disentangle overlapping ESR spectra. The feasibility of this method in a modified commercial X-band spectrometer has been demonstrated by Granwehr et al. [14,15]. Continuous LOD spectrometers use a deep *rf* modulation of the microwave excitation with frequency Ω. A less common alternative is the microwave irradiation of the sample with two coherent microwave sources with a frequency difference of Ω. In both methods an oscillation of M_z is induced with the fundamental and harmonic frequencies of Ω [9]. A detection coil, that is parallel to the longitudinal magnetization and is part of a resonant circuit, is tuned to one of the harmonics of Ω. It has been shown by Herve and Pescia [17] that a phase sensitive detection of the induced voltage allows the measurement of T_1. An instrument operating in X-band with a resonant microwave cavity and a relatively low microwave power has been developed by Atsarkin et al. [11]. To complement the original phase method of [17], Atsarkin et al. developed an amplitude version also that enables measurement of T_1 even when $T_1 \ll \Omega^{-1}$ by comparing the cw LOD-ESR and cw ESR spectra. The primary use of our apparatus is the detection of T_1 using the phase version. In the simplest case [9,11,17] when $\Omega \cdot T_1 < 1$, the ratio of the in (u) and out-of phase (v) components of the oscillating magnetization gives:

$$T_1 = \frac{1}{\Omega} v/u. \tag{1}$$

The LOD-ESR spectrum is distorted when $\Omega \cdot T_1 > 1$ and this simple equation no longer holds. Often, $T_1 \simeq T_2$ and the most visible consequence of higher modulation frequencies is the distortion of the LOD signal at the Ω sidebands of the microwave radiation [15]. We developed a numerical method to solve the Bloch equations for the cw LOD-ESR case with arbitrary T_1, T_2, and Ω. As shown below, this enables to determine T_1 and T_2 independently in wide range of Ω, T_1, and T_2.

3. The LOD spectrometer

The deep amplitude PIN diode modulation of the microwave field and the use of a sample holder or microwave cavity that enables the detection of the induced voltage in a pick-up coil are the main difference between conventional cw and LOD-ESR spectrometers. We do not employ a resonant microwave structure in our design. The advantages are: broadband exciting microwave operation, larger useful sample quantity, less limitation on the modulation *rf* bandwith, simpler design for transparency of the *rf* field from the sample to the detection coil. The reduced sensitivity due to the low (typically 10^{-5}) saturation factor ($s = \gamma_e^2 B_1^2 T_1 T_2$) is the main disadvantage. A resonant structure would increase the LOD-ESR signal proportionally to the quality factor.

The block-diagram of the spectrometer is shown in Fig. 1. The HF-LOD-ESR is based on a high homogeneity (10 ppm/cm) superconducting magnet (Oxford Instruments 0–9 T) equipped with a cryostat for the 1.5–400 K temperature range that is regularly used for cw HF-ESR measurements. The 35 GHz microwave source is a Gunn diode (Farran Technology GV-28 M, $f_0 = 35.4$ GHz) with an ouput power of 150 mW and automatic frequency controlled to an external ambient temperature cavity. Outside the magnet, the 35 GHz microwaves propagate in a WR-28 waveguide (waveguide A) and are then fed through a rectangular to circular feedhorn into an oversized (8 mm diameter) circular stainless steel waveguide (waveguide B) in the cryostat of the magnet. The 75 GHz microwave source is a quartz oscillator stabilized Gunn diode (Radiometer Physics) with 50 mW power which is directly fed into the oversized waveguide. The 8 mm circular waveguide allows only the circular TE11 mode at 35 GHz, whereas at 75 GHz there is a mixture of several waveguide modes. The loss of the microwave intensity from the microwave sources to the sample is approximately 10 dB at 35 GHz and 6 dB at 75 GHz, corresponding to $B_1 = 16$ mG and $B_1 = 14$ mG, respectively. The microwave power is amplitude modulated by PIN diodes (Millitech PSH-28, power switching speed: 10–90%, 1.5 ns; 90–10%: 1 ns at 35 GHz and Millitech PSP-12, power switching speed: 10–90%, 150 ns; 90–10%: 20 ns at 75 GHz) that are driven by a high frequency *rf* lock-in amplifier (Stanford

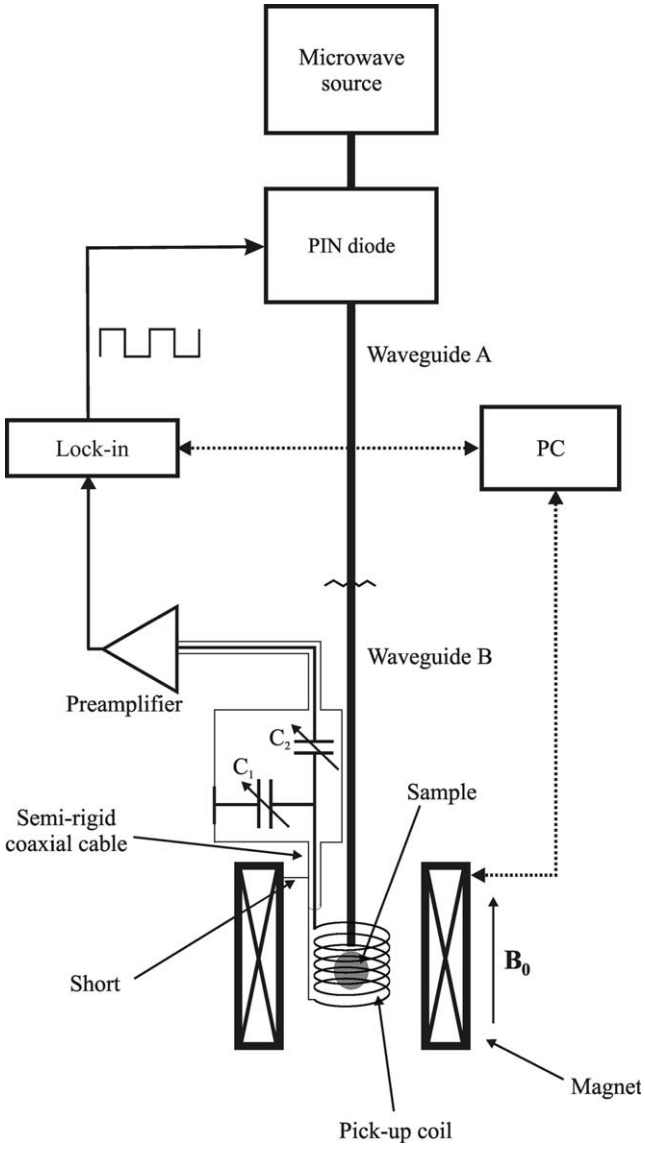

Fig. 1. Block diagram of the HF-LOD-ESR spectrometer. The waveguide changes from WR-28 (waveguide A) to an 8 mm stainless steel tube for 35 GHz (waveguide B) and it is an 8 mm tube throughout at 75 GHz.

Research Systems, SRS844, 0.025–200 MHz). These switching speeds allow 80 and 2 MHz maximum microwave power modulation frequencies at 35 and 75 GHz, respectively.

The sample is placed in an 8 mm diameter thin walled brass sample holder with a vertical slit. This construction suppresses eddy currents in the walls and along the circumference of the sample holder. *rf* eddy currents reduce the amplitude and shift the phase of the voltage induced by the oscillating magnetization of the sample. Brass (CuZn39Pb3) rather than high purity copper is used as it has a larger, temperature independent resistivity. The resonant circuit is similar to those commonly used in NMR spectrometers [18,19]. The coil is part of a resonant *rf* circuit and is fixed with epoxy resin. It contains a few turns of 1 mm diameter copper wire and is wound around the brass sample holder. The typical inductivity of the coil is 1–20 μH. There are two capacitors: one for frequency tuning (C_1) that is parallel to the coil and an impedance matching serial one, C_2. Both capacitors are tunable and are suited for cryogenic and high magnetic field applications (C_1: 5–120 pF Voltronics NMTM120 CEK, C_2: 2–70 pF, Voltronics NMTM70 CEK). Similarly to the NMR instrumentation, the resonance circuit has to be tunable, and for maximum power transfer the impedance of the *rf* circuit should match the input impedance of the preamplifier.

Placed near the coil in the cryostat, the capacitors allow to vary the modulation frequency by approximately a factor of 2 without changing the pick-up coil. When capacitors are outside the magnet, the highest available frequency is limited by the parallel capacitance of the 50 Ω coaxial cable leading to the coil but there is no lower limit on the frequency as capacitors can be freely changed. The performance of the apparatus is best when the impedance of the the coil is $L\Omega \simeq 50\,\Omega$ similarly to the common rule of NMR instrumentation [18]. In order to satisfy this, we constructed a series of sample holders with mounted-on coils for the frequency bands: 2–3, 7–9, 15–18, 20–24 MHz. We observed a significant (up to 50 pF) stray capacitance between the grounded brass sample holder and coils operating in the lowest *rf* frequency range. This, however, does not affect the performance of the apparatus.

The *rf* circuit is matched to the 50 Ω input of a low noise preamplifier (Analog Modules 322-6-50, 200 Hz–100 MHz, gain 40 dB, input noise 380 pV/$\sqrt{\text{Hz}}$) that is followed by phase sensitive detection with a SRS-844 lock-in amplifier (bandwidth: 0.025–200 MHz, noise: 5 nV/$\sqrt{\text{Hz}}$) that also drives the amplitude modulation. Data readout from the lock-in and all other parameters of the spectrometer, such as the magnetic field sweep and temperature settings are computer controlled. The overall noise figure of the set-up when capacitors are placed near the sample is less than 1 nV/$\sqrt{\Delta f}$, where Δf is the bandwidth of the lock-in. This is close to the theoretical Johnson noise of a 50 Ω resistance at room temperature. The overall noise figure is unaffected by the quality factor $Q_{RLC} = \frac{1}{R}\sqrt{\frac{L}{C}}$ of the resonant circuit, where R is the resistance of the coil at the *rf* frequency. The disadvantage of placing the capacitors in the cryostat is that they are strongly temperature dependent and have to be retuned when temperature is changed. The noise is increased by a factor of 1.5 when the capacitors are outside the magnet but in this configuration resistivity changes of the pick-up coil detune the *rf* circuit less. Another practical advantage of this set-up is that capacitors can be removed and the *rf* pick-up coil may be used for magnetic field modulation when conventional cw ESR measurements are run.

The isolation of the *rf* circuit from external *rf* sources is a general problem of detection at $1\,\mathrm{nV}/\sqrt{\Delta f}$ noise level. The PIN diode driven at the same frequency as the detection is a powerful *rf* source radiating near the detector. One way of suppressing the resulting noise is *rf* detection at the second harmonic of the modulation frequency. As this reduces the signal, we operate our apparatus at the fundamental harmonic of the modulation. The preamplifier and the PIN diode are embedded together with their dc power supplies (storage batteries) in separate Faraday cages providing good radiation protection. In the room temperature capacitor version, the capacitors are in a common housing with the preamplifier. The coaxial cables leading to and from the Faraday cages are double shielded. Thermometers and heating wires inside and outside the magnet are also isolated from the *rf* circuit. One end of the coil and C_1 are grounded to the magnet (Fig. 1). The latter is grounded through the preamplifier to the input of the *rf* lock-in. The PIN diode is also grounded to the output of the lock-in. The rest of the microwave bridge is electrically isolated from the ground. This ensures good radiation suppression and prevents ground loops. The residual radiative coupling is in the range of a few 100 nV. This is the order of magnitude specified for the *rf* lock-in and results mainly from the internal radiation between its input and output. It does not increase the overall noise of the apparatus but results in a magnetic field independent constant background. Optionally, we can remove at 35 GHz the background with a double lock-in technique: in addition to the *rf* amplitude modulation, the microwaves are modulated at low frequency, $f < 100$ Hz, using a secondary low switching speed PIN diode (Millitech PSP-28, switching speed: 10–90%, 150 ns; 90–10%: 20 ns) that is driven by an external waveform source. Two identical low frequency lock-ins (SRS830, 0.001 Hz–102 kHz) are connected to the X and Y outputs of the *rf* lock-in and are locked to the external waveform source. The double amplitude modulation reduces the microwave intensity and thus the LOD signal by a factor of two. The bandwidth of the rf lock-in is increased for the double modulation and it is used as a heterodyne demodulator and the bandwidth is set on the two low-frequency lock-ins. Magnetic field modulation would be an alternative to double amplitude modulation but here *rf* radiation shielding is more difficult.

4. Operation of the LOD-ESR spectrometer

The primary purpose of the LOD spectrometer is to determine T_1 as a function of temperature by a phase sensitive detection of the dynamic magnetization. Various elements such as cables, the PIN diode, waveguides, *rf* circuit, and the preamplifier result in a significant instrumental phase shift between the driving reference and the detected signal. Below, we describe how the instrumental phase shift can be separated from the one due to the sample. The absolute phase error of the *rf* lock-in [22] depends on the *rf* modulation frequency, but does not vary with time and is less than 2 degrees and is included in the instrumental phase shift also. The frequency dependence of the instrumental phase shift, 15°/MHz, requires operation at fixed frequency. The lock-in provides a very stable *rf* source with a long term frequency stability of 5 ppm. The phase shift of the 50 Ω matched *rf* circuit depends sensitively on how well it is tuned to resonance. For tuning, the signal reflected from the *rf* circuit at the working frequency is compared to the signal reflected from a resistive 50 Ω using a 180° hybrid Tee (MA-COM Model HH-107, 2–200 MHz). This limits the lowest modulation frequency of our apparatus to 2 MHz. This procedure is well known in NMR instrumentation. To improve the reproducibility and simplify the operation, an *rf* switch redirects the driving signal of the PIN diode toward the hybrid Tee and the 50 Ω, this allows us to tune the *rf* circuit without cable replacement between tuning and measurement. When the temperature of the sample is changed, the detuning of the *rf* circuit is monitored and it is retuned to 50 Ω within $\pm 0.5\%$ that results in a $\pm 1°$ uncertainity of the phase. This, together with the $\pm 1°$ relative phase error [22] of the *rf* lock-in between the two channels, gives $\pm 2°$ phase error. This is a systematic error of our apparatus that limits the T_1 measurement. We find numerically that this phase error is smallest when $0.8 < \Omega T_1 < 1.2$ and then $\Delta T_1/T_1 \approx 13\%$. This determines the optimum modulation frequency for the measurement of T_1. When the optimal modulation condition can not be satisfied the measurement of T_1 is less precise: $\Delta T_1/T_1 \approx 18\%$ when $2.0 < \Omega T_1 < 2.2$ and $\Delta T_1/T_1 \approx 24\%$ when $0.2 < \Omega T_1 < 0.4$.

We determined the instrumental shift for a few fixed *rf* frequencies from measurements on a sample with a known value of T_1. This can be used thereafter to determine T_1 in samples with unknown spin–lattice relaxation. We used RbC_{60} as reference material (see below) for which the room temperature T_1 and T_2 measured at 3.5 GHz are equal. The 1.5 ns 10–90% switching time of the PIN diode limits the measurable T_1 range to $T_1 \gtrsim 2$ ns, corresponding to a 28 G homogeneous linewidth at 35 GHz. The T_1 measurement is currently limited to $T_1 \gtrsim 20$ ns at 75 GHz. The maximum detectable $T_1 \approx 80$ ns, is limited by the 2 MHz lowest modulation frequency.

From the theory of LOD-ESR [9,17] the amplitude of the detected voltage is

$$V = kNA\mu_0 M_0 \Omega \frac{\gamma_e^2 B_1^2 T_1 T_2}{\pi\hbar^2\sqrt{1+\Omega^2 T_1^2}}, \tag{2}$$

where k is the volume filling factor of the pick-up coil, N is the number of turns of the coil, A is the cross section of the coil, γ_e is the electron gyromagnetic ratio, M_0 is

the equilibrium magnetization, B_1 is the magnetic component of the microwave field. We follow some simple steps in designing the geometry for a particular measurement. As discussed above, the condition for optimal performance of the apparatus is $\Omega_{\text{optimal}} T_1 \approx 1$. Together with the $L\Omega \simeq 50\,\Omega$ condition, this determines the impedance of the pick-up coil.

The overall sensitivity is given by

$$S = V/n, \tag{3}$$

where n is the number of spins. Under optimal conditions ($T_1 \sim T_2 = 1/\gamma_e \Delta H$, $\Omega_{\text{optimal}} \propto \Delta H$, and $N \propto 1/\sqrt{\Omega_{\text{optimal}}}$) the sensitivity is $S \sim 1/\Delta H^{3/2}$. However, the sensitivity decreases with the square of the homogeneous linewidth when $1/T_1$ is longer than the maximum modulation frequency. The relatively low sensitivity of our apparatus may be compensated with the use of larger sample mass provided it does not significantly absorb the microwave power. A resonant microwave structure with a moderate quality factor such as $Q = 100$ or the use of microwave power amplifiers could also increase the sensitivity of our HF-LOD-ESR apparatus.

5. Measurement of T_1 in RbC_{60}

We demonstrate the performance of the apparatus by a T_1 measurement of a RbC_{60} sample above the Neél temperature $T_N = 35\,K$. RbC_{60} is a conducting alkaline fulleride polymer in its normal state, above 50 K [20]. Orthorhombic RbC_{60} consists of parallel running charged fulleride chains with a possibly quasi 1D electronic structure [26]. In its ground state RbC_{60} is an antiferromagnetic insulator. Above the Neél temperature, a gradual insulator to metal transition occurs with strong 3D fluctuations up to 50 K. Above 50 K it is a poorly conducting normal metal. The loose, 20 mg, powder sample was in a 10 mm high teflon sample holder. The optimal impedance of the 9 mm diameter, $N = 13$ turns coil, wound around the waveguide is $L = 1\,\mu H$. The relatively small RbC_{60} sample has a low filling factor of $k = 0.016$. The spin susceptibility of RbC_{60}, $\chi \approx 10^{-3}$ emu/mol [21] is nearly temperature independent. At room temperature $T_1 \approx T_2 \approx 13.2$ ns (see below) and at the *rf* modulation frequency $\Omega_2 = 7.49$ MHz [25]. $V = 70$ nV detected voltage from Eq. (2) and a signal-to-noise ratio of 70 is expected after the $1\,nV/\sqrt{\Delta f}$ low noise preamplifier. A similar calculation at 75 GHz and $\Omega_2 = 1.95$ MHz, near the upper limit of the 75 GHz PIN diode, yields $V = 75$ nV. These results agree with the experimentally determined 100 and 70 nV at 35 and 75 GHz, respectively. The measured overall sensitivity is $S = 3.3 \times 10^{16}$ spin/$G^{3/2}$ at 35 GHz and similarly $S = 1.2 \times 10^{16}$ spin/$G^{3/2}$ at 75 GHz.

In Fig. 2, we show the phase sensitively detected HF-LOD-ESR spectra of RbC_{60} at 60 and 290 K detected at 35 GHz microwave and 2.9 MHz *rf* frequency. The LOD signal is corrected for the temperature independent instrumental angle discussed above. The intensity ratio of the in- and out-of phase LOD signals changes with temperature: $v/u = 0.25$ and $v/u = 0.84$ at 290 and 60 K, respectively. Under these conditions, the $v/u = \Omega T_1$ approximation is valid and we obtain $T_1 = 14$ and 46 ns at 290 and 60 K, respectively. Fig. 3. demonstrates the changes of the LOD-ESR lineshape when the *rf* modulation frequency is increased from 2.9 to 15.9 MHz. The gradual broadening of the LOD-ESR signal and the appearance of sidebands at Ω are characteristic of the breakdown of the $v/u = \Omega T_1$ approximation when $\Omega T_1, T_2 \gtrsim 1$. In Fig. 3, we show fits to the observed lineshapes. Here, we optimized the parameters T_1, T_2 using numerical solutions of the Bloch equations. This fitting procedure allows a better determination of T_1 as all points of the spectra are taken into account in the calculation. The power at the microwave sidebands is different as a result of standing waves caused by the unmatched microwave load in the oversized waveguide. This results in a small but observable asymmetry of the HF-ESR-LOD spectra. We took this effect into account in the determination of T_1.

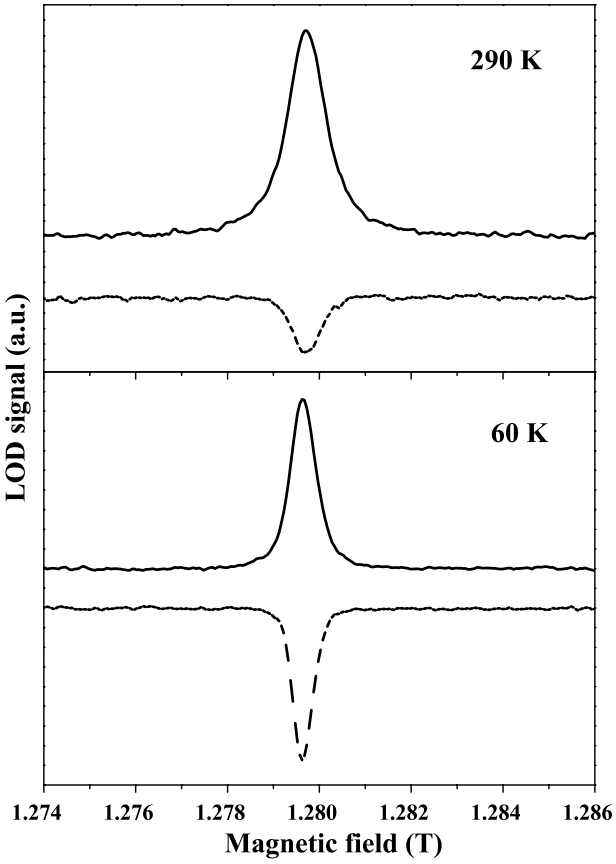

Fig. 2. Phase sensitively detected HF-LOD-ESR spectra of RbC_{60} at 35 GHz and $\Omega/2\pi = 2.9$ MHz at 60 and 290 K (solid line: in-phase, dashed line: out of phase signal). The phase shift is related to the temperature dependence of T_1.

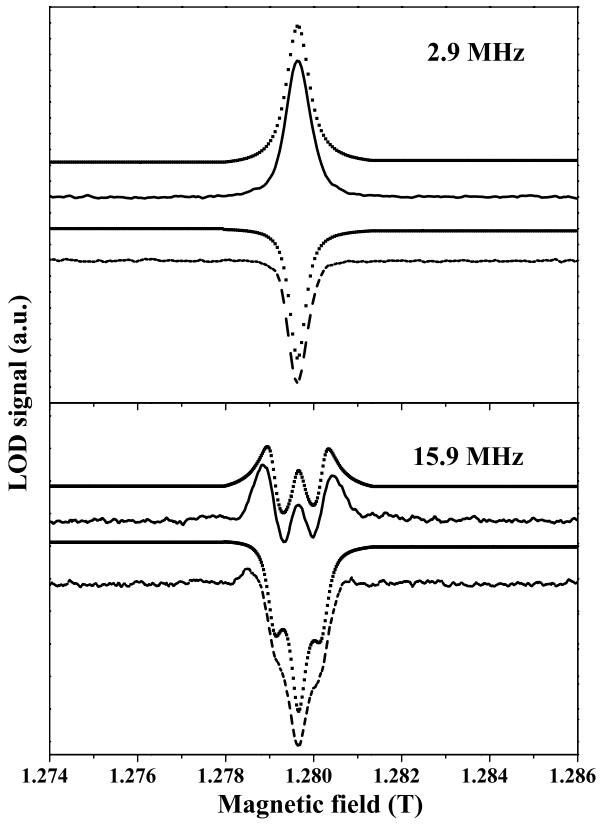

Fig. 3. HF-LOD-ESR spectra of RbC_{60} at 35 GHz and 60 K at $\Omega/2\pi = 2.9$ MHz and 15.9 MHz. Dotted curves show fits as explained in the text with $T_1 = 46$ ns (solid line: in-phase, dashed line: out of phase signal).

In Fig. 4, we show the temperature dependent T_1 determined at 2.9 and 7.49 MHz at 35 GHz microwave frequency, using the above described numerical method, together with T_2 determined from the cw ESR linewidth at 3.5 GHz. The partially averaged g-factor anisotropy of RbC_{60} [20,27,28] gives rise to a small, magnetic field dependent contribution to the linewidth, the inverse linewidth approximates $\gamma_e T_1$ at the small magnetic fields of the 3.5 GHz measurement. The T_1 data were determined after correcting for the temperature independent instrumental phase shift as described above. This procedure assumes equal T_1 and T_2 values at 290 K. T_1 values determined this way are remarkably similar at 2.9 and 7.49 MHz *rf* frequencies in the whole temperature range, although T_1 changes by a factor of $\sim$3 from 290 to 60 K. The T_1 and T_2 data agree above 150 K within experimental precision and show similar temperature dependences but they are somewhat different below this temperature. Temperature dependence of the instrumental phase shift can be ruled out as it would give rise to different deviations at 2.9 and 7.49 MHz *rf* frequencies but this is not observed. A more likely alternative is the break-down of the often assumed $T_1 = T_2$ relation. This law relies on cubic symmetry [23] while RbC_{60} is a quasi one-dimensional conducting polymer with anisotropic properties.

As shown in Fig. 4, both T_1 and T_2 become longer on lowering the temperature from 290 to 50 K, as in a conventional metal [24]. However, both quantities show a downturn in the range of 50–35 K, just above the 3D ordering transition of RbC_{60} [20]. The downturn of the field independent part of T_2 below 50 K was assigned to the onset of three-dimensional precursor fluctuations of the 35 K SDW transition of RbC_{60} [20]. Our direct measurement of T_1 shows that there is an increase of the relaxation rate with the slowing down of fluctuations. This confirms the earlier assignment of ESR line broadening to fluctuations in a relatively broad temperature range between 35 and 50 K.

In Fig. 5. we demonstrate the performance of our apparatus at 75 GHz microwave frequency. A full investigation at this frequency of RbC_{60} was not possible because of the slower switching times.

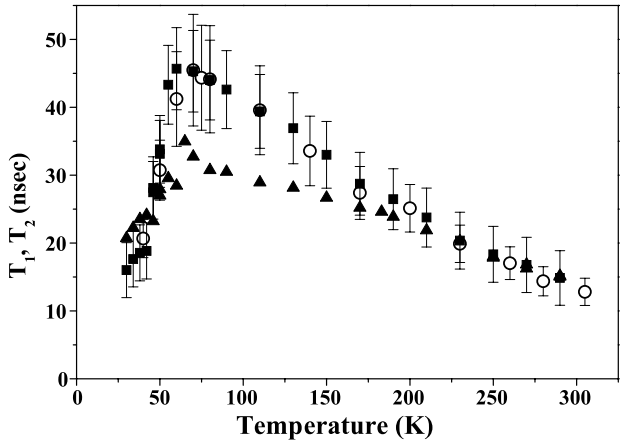

Fig. 4. Temperature dependence of T_1 at 2.9 (■) and 7.49 MHz (○) *rf* and 35 GHz microwave frequency and T_2 determined from the cw-ESR linewidth at 3.5 GHz (▲).

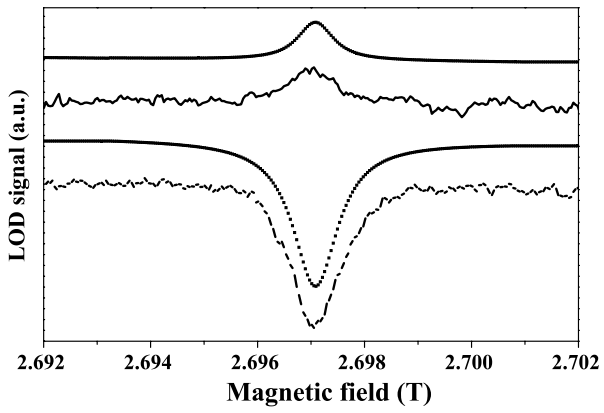

Fig. 5. HF-LOD-ESR spectra of RbC_{60} at 75 GHz and 290 K at $\Omega/2\pi = 1.95$ MHz. Dotted curves show fits as explained in the text (solid line: in-phase, dashed line: out of phase signal).

6. Conclusion

In conclusion, we presented the construction and the performance of a high frequency longitudinally detected ESR spectrometer. Operation at different microwave frequencies is possible as no resonant microwave elements are used. The spectrometer uses commercially available elements mainly and its adaptation to HF-ESR instruments is straightforward. The multifrequency design enables the study of magnetic field or frequency dependent relaxation phenomena. The primary use of the spectrometer is to study relaxation with T_1 in the 2–80 ns range. We discussed the measurement of T_1 in the RbC_{60} alkali fulleride conducting polymer.

Acknowledgments

The authors would like to express their gratitude to L. Forró for providing the RbC_{60} sample, V.A. Atsarkin, Gy. Kriza, P. Matus, and J. Granwehr for fruitful discussions on the experimental setup. Support from the Hungarian State Grants, OTKA T043255, OTKA TS040878, OTKA NDF45172, and FKFP 0352/1997 are acknowledged. FS acknowledges the Bolyai Hungarian Research Fellowship for support and the hospitality of the University of Wien during the preparation of the manuscript.

References

[1] J.H. Freed, Ann. Rev. Phys. Chem. 51 (2000) 655.
[2] A.K. Hassan, L.A. Pardi, J. Krzystek, A. Sienkiewicz, P. Goy, M. Rohrer, L.-C. Brunel, J. Magn. Res. 142 (2000) 300.
[3] O. Burghaus, M. Rohrer, T. Götzinger, M. Plato, K. Möbius, Meas. Sci. Technol. 3 (1992) 765.
[4] J.P. Barnes, J.H. Freed, Rev. Sci. Instrum. 69 (1998) 3022.
[5] G.M. Smith, J.C.G. Lesurf, R.H. Mitchell, P.C. Riedi, Rev. Sci. Instrum. 69 (1998) 3924.
[6] J.A.J.M. Disselhorst, H. van der Meer, O.G. Poluektov, J. Schmidt, J. Magn. Reson. 116 (1995) 183.
[7] F. Simon, A. Jánossy, F. Murányi, T. Fehér, H. Shimoda, Y. Iwasa, L. Forró, Phys. Rev. B 61 (2000) 3826.
[8] F. Simon, A. Jśnossy, T. Fehér, F. Murányi, S. Garaj, L. Forró, c. Petrovic, S.L. Bud'kor, G. Lapertot, V.G. Kogan, P.C. Canfield, Phys. Rev. Lett. 87 (2001) 047002.
[9] J. Pescia, Ann. Phys. 10 (1965) 389.
[10] T. Strutz, A.M. Witowski, R.E.M. de Hekker, P. Wyder, Appl. Phys. Lett. 57 (1990) 831.
[11] V.A. Atsarkin, V.V. Demidov, G.A. Vasneva, Phys. Rev. B 52 (1995) 1290.
[12] G. Ablart, J. Pescia, S. Clement, J.P. Renard, Solid State Commun. 45 (1983) 1027.
[13] M. Martinelli, L. Pardi, C. Pinzini, S. Santucci, Solid State Comm. 17 (1975) 211.
[14] J. Granwehr, A. Schweiger, Appl. Magn. Res. 20 (2001) 137.
[15] J. Granwehr, J. Forrer, A. Schweiger, J. Magn. Res. 151 (2001) 78.
[16] The most commonly used frequency of our apparatus, 35 GHz, is conventionally not yet considered as HF-ESR. We use the HF-ESR terminology as the lack of resonant microwave structures allows a straightforward extension to higher frequencies.
[17] J. Herve, J. Pescia, C.R. Acad. Sci. (Paris) 251 (1960) 665.
[18] W.G. Clark, J.A. McNail, Rev. Sci. Instrum. 44 (1973) 844.
[19] D.I. Hoult, R.E. Richards, J. Magn. Res. 24 (1976) 71.
[20] A. Jánossy, N. Nemes, T. Fehér, G. Oszlányi, G. Baumgartner, L. Forró, Phys. Rev. Lett. 79 (1997) 2718.
[21] O. Chauvet, G. Oszlányi, L. Forró, P.W. Stephens, M. Tegze, G. Faigel, A. Jánossy, Phys. Rev. Lett. 72 (1994) 2721.
[22] See the manual of the SRS844 lock-in. Available from http://www.srsys.com/html/sr844.html.
[23] Y. Yafet, Solid State Physics, Academic Press, 14 (1963) 1.
[24] R.J. Elliott, Phys. Rev. 96 (1954) 266.
[25] The $\Omega T_1 \approx 1$ condition gives an optimal 12 MHz for this relaxation time.
[26] P.W. Stephens, G. Bortel, G. Faigel, M. Tegze, A. Jánossy, S. Pekker, G. Oszlányi, L. Forró, Nature (London) 370 (1994) 636.
[27] J. Rahmer, A. Grupp, M. Mehring, J. Hone, A. Zettl, Phys. Rev. B 63 (2001) 081108(R).
[28] J. Rahmer, A. Grupp, M. Mehring, Phys. Rev. B 64 (2001) 235405.